Predicting the thermal performance of thermochromic flat plate solar collectors

Predicting the thermal performance of thermochromic flat plate solar collectors

Anna Krammer, Andreas Schüler

Solar Energy and Building Physics Laboratory LESO-PB, EPFL, Station 18
CH-1015 Lausanne, Switzerland

anna.krammer@epfl.ch

Abstract. A thermochromic vanadium dioxide (VO_2) based absorber coating is proposed. The optical response of the multilayered absorber is first simulated, then, the spectral reflectance of the deposited absorber is measured. The determined solar absorptance and thermal emittance values are used to predict the thermal performance of the thermochromic flat plate solar collector. The corresponding stagnation temperature is estimated to be ~25°C lower than that of a standard collector. This is mostly due to the increase in emissivity over the thermochromic phase transition and, partially, to a lower solar absorptance than in standard absorbers. However, a concurrent increase of the solar absorptance over the phase transition limits the overheating protection abilities of the thermochromic collector. Alternative scenarios based on thermochromic absorbers with assumed, constant solar absorptances and the same temperature dependent thermal emittance as determined for the measured sample, are considered. The corresponding thermal performances and stagnation temperatures are predicted and discussed.

1. Introduction

A novel smart, thermochromic solar absorber has been developed. Its particularity lays in the ability to change its optical properties with temperature. At normal operating temperatures the thermochromic absorber exhibits a high solar absorptance and low thermal emittance, while at high operating temperatures the thermal emittance is increased drastically. In this fashion, it provides a passive overheating protection of the solar collector.

An inorganic thermochromic material, undergoing a first order semiconductor-to-metal phase transition is vanadium dioxide. The perfectly reversible transition occuring at 68°C, with a transition temperature adjustable by doping, makes VO_2 a promising choice for solar thermal applications.[1] Through the thermochromic transition, the optical properties of the film change markedly – especially in the near and mid-infrared spectral region – and a thermal emittance modulation of ~25 – 30% has been reported for individual thermochromic films deposited on Al substrates[2].

The aim of this study is to predict the thermal performance of a thermochromic flat plate solar collector and compare it with the performance of standard solar collectors. First, a multilayered absorber design is proposed consisting of an infrared reflective aluminum substrate, a VO_2 thin film, a spinel $CuCoMnO_x$ selective absorber and a SiO_{2-x} antireflective top layer. The optical performance of the absorber is evaluated based on the n and k optical constants and thicknesses of the constituting layers. Then, according to the suggested multilayered design, lab-scale thermochromic absorber coatings are prepared. The experimentally determined solar absorptance and thermal emittance values are fed into a

numerical simulation model (SolCoSi)[3] in order to predict the thermal efficiency curve and the stagnation temperature of the thermochromic collector.

2. Experimental methods

2.1. Sample deposition

All oxide films are deposited by high-vacuum, reactive magnetron sputtering. The base pressure in the chamber is below $5 \cdot 10^{-8}$ mbar. Argon serves as process gas, O_2 is the reactive gas for oxide formation. The multilayered absorber stack is deposited on 50 mm x 50 mm large and 0.5 mm thick Al sheets. Thermochromic VO_2 is very sensitive to fluctuations in oxygen partial pressure during the sputtering process. A Proportional Integral Derivative (PID) feedback control regulates the oxygen flow based on the pressure readings of a lambda-probe oxygen sensor. For the other oxide films, controlling the oxygen flow with a mass flow controller is sufficient. For uniform film deposition, all samples are rotated at 20 rpm. The VO_2 and $CuCoMnO_x$ spinel films are deposited at high temperature, T_{dep} =600°C measured by a stationary thermocouple above the rotating substrate holder.

The VO_2 film is deposited at a working pressure of $7.15 \pm 0.05 \cdot 10^{-3}$ mbar, with an O_2 to Ar ratio of 1:12.3(± 0.5). The $CuCoMnO_x$ is sputtered at $\sim 4 \cdot 10^{-3}$ mbar (1:3.2 O_2 to Ar ratio), while the SiO_{2-x} film at $7 \cdot 10^{-3}$ mbar (1:21 O_2 to Ar ratio).

2.2. Sample characterization

The total reflectance of the multilayered absorbers is measured over the 0.36 – 14 μm spectral range. In the visible 0.36 – 0.8 μm range, a LOT, RT-060-SF integrating sphere, an Oriel MultiSpec 125TM 1/8m spectrometer and an Instaspec Silicon Photodiode Array Detector are used. In the near-infrared range (0.8 -2.5 μm) a monochromator (Optronic Laboratories, OL 750-MPS) associated with a NIR-sensitive PbS detector (Optronic Laboratories, OL 730) is employed. Finally, in the Mid-IR range (2.5 - 14 μm) the reflectance is measured with a Bio-Rad FTS-175C Fourier transform infrared spectrometer equipped with a 3" gold coated integrating sphere and a nitrogen-cooled MCT detector.

The solar absorptance, α_{sol} is determined from the total spectral reflectance measured over the 0.36 - 2.5 μm range and calculated with the ASTM G173-03 reference spectra. In the thermal-infrared region, the spectral emissivity for opaque materials can be expressed in terms of total spectral reflectance using Kirchhoff's law:

$$\varepsilon(\lambda) = \alpha(\lambda) = 1 - \varrho(\lambda),$$

where $\varepsilon(\lambda)$ is the spectral emissivity, $\alpha(\lambda)$ the spectral absorptivity and $\varrho(\lambda)$ the spectral reflectivity. By weighting the total spectral emissivity (measured over the 2.5 – 14 μm spectral range) with the black body radiation of a body at T = 373 ° K, the thermal emittance of the absorber, ε_{th} is determined.

2.3. Simulation of absorber and collector performance

The optical response of the envisaged multilayered absorber is calculated based on the transfer-matrix method, starting from the n and k optical constants and thicknesses of the individual oxide films. The optical constants used for the simulation are adopted from literature (from [4] VO_2 in both the cold and hot state, from [5] for $CuCoMnO_x$, and Semilab SEA ellipsometry database for the Al substrate and SiO_2), therefore, some variation between the simulated and measured optical behavior is expected.

The simulated or measured α_{sol} and ε_{th} are introduced into a numerical simulation model (SolCoSi), which predicts the thermal performance of flat plate solar collectors. The simulation is based on a nodal model proposed by Garcia-Valladares and Velazquez[6], which combines the multilayer method of Cadafalch[7] with a discretization also in the longitudinal direction. The simulation takes into account the following assumptions: control volume discretization in the axial and longitudinal directions, steady state conditions, temperature-dependent thermophysical properties, conductive heat transfer in solids and convective heat transfer in fluids.[3] In this work, the parameters of a standard flat plate collector, with a single glass cover and aluminum absorber are considered.

3. Results and discussion

The proposed thermochromic absorber, A1 consists of an infrared reflective aluminum substrate, a ~210 nm VO_2 thin film, a 20 nm spinel $CuCoMnO_x$ selective absorber and a 40 nm SiO_{2-x} antireflective top layer.

The schematic of the absorber design and the experimentally determined spectral reflectance curves, measured both at room temperature and at 100°C, are displayed in Fig. 1. The corresponding solar absorptance, α_{sol} and thermal emittance, ε_{th} are summarized in Table 1 and compared with the values expected from the multilayer simulation. The measured solar absorptance values, α_{sol} are higher than those predicted: ~ 7% higher in the room temperature state and ~4% higher at 100°C. Nevertheless, both simulation and measurement corroborate an increase in α_{sol} over the thermochromic transition of 10% and 7%, respectively. Concerning the thermal emittance, in the room temperature state the simulated and measured values are rather consistent with 7% simulated emittance compared to 9% measured. However, in the high temperature state the simulated and measured emittances diverge significantly from 20% to 40%. This considerable difference suggests that the optical constants determined for the VO_2 film in its high temperature state might not describe adequately the multilayer's response. This might arise from the inferior VO_2 film purity deposited in this work. The optical constants have been determined for high quality, pure VO_2 films, whereas, due to the challenges in maintaining a very narrow oxygen partial pressure range during deposition, some V_2O_3 or V_2O_5 might be also present in the thermochromic film. Even small amounts of other vanadium oxides could considerably increase the emissivity in the high temperature state (in the low temperature state the films are transparent and the IR reflective Al substrate is governing the multilayer response). For solar thermal applications, where at high operating temperatures a high thermal emittance is desired, these increased emittance values are favorable.

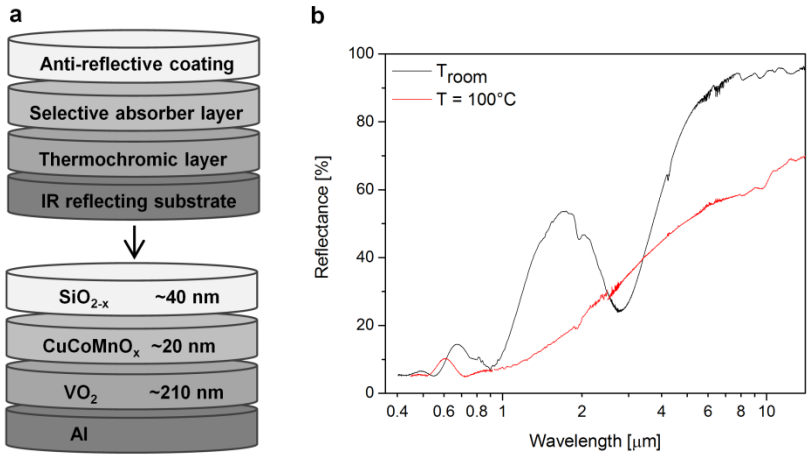

Figure 1. (a) Schematic drawing of the multilayered solar absorber coating, A1 and proposed film thicknesses. (b) Spectral reflectance of the thermochromic absorber measured in the 0.4 – 14 μm range both below, at T_{room}, and above the thermochromic transition, at T = 100°C.

Table 1. Simulated and measured solar absorptance and thermal emittance of the multilayered absorber coating.

	α_{sol}		ε_{th}		$\Delta\alpha$	$\Delta\varepsilon$	ΔTot
	T_{room}	T = 100°C	T_{room}	T = 100°C			
Simulated A1	0.77	0.87	0.07	0.21	-0.10	0.14	0.04
Measured A1	0.84	0.91	0.09	0.40	-0.07	0.31	0.24
Projected A2	0.84	0.84	0.09	0.40	0	0.31	0.31
Projected A3	0.95	0.95	0.09	0.40	0	0.31	0.31

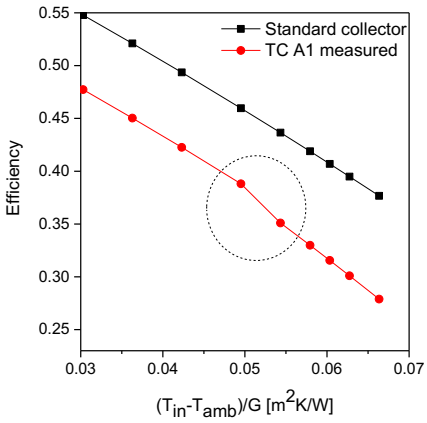

Figure 2. Efficiency curves of a standard flat plate collector and a thermochromic collector based on absorber A1. The circle marks the drop in efficiency attributed to the thermochromic phase transition occurring at ~67°C. (T_{in} is the inlet fluid temperature, T_{amb} the ambient temperature, G the incident solar radiation.)

With the determined α_{sol} and ε_{th} values for absorber A1, the thermal efficiency curve of a thermochromic collector has been determined based on the inlet fluid temperature T_{in}, and collector aperture area. For comparison, the efficiency of a collector based on standard selective absorber with 0.95 absorptance and 0.05 emittance is plotted. The results are shown in Fig. 2. The efficiency of the standard collector is constantly decreasing with increasing fluid temperature. The thermochromic collector exhibits a similar trend with a small, but sudden decrease in efficiency occuring at the thermochromic phase transition temperature, where the emittance of the absorber suddenly increases. The calculated stagnation temperature is 177°C for the standard collector and 152°C for the thermochromic collector (Table 2). The 25°C decrease in stagnation temperature is mostly due to the excellent thermal emittance modulation, $\Delta\varepsilon$ of 0.31 for absorber A1 and it happens in spite of a 0.07 increase in solar absorptance over the thermochromic transition. Another contributing factor, is the slightly lower α_{sol} of the thermochromic absorber in the high temperature state compared to that of a standard absorber. At normal operating temperatures, the α_{sol} of the thermochromic absorber is even more modest and considerably limits the collector performance. Nonetheless, the important reduction of 25°C, shortens significantly the duration of stagnation conditions, prevents the evaporation of the heat transfer medium and the decomposition of glycols.

A collector A2 is imagined, based on a thermochromic absorber where the solar absorptance, α_{sol} = 0.84 stays constant over the transition. The thermal emittance values are assumed to be the same as for absorber A1. Then, the two thermochromic collectors A1 and A2 show identical efficiency curves below the thermochromic transition temperature. However, above the phase transition, the efficiency of collector A2 is decreasing more drastically as the emittance modulation manifests its effects more clearly in the absence of an increase in solar absorptance. (Fig. 3) The new stagnation temperature determined for the collector A2 is 147°C. Below ~150°C and at 2 bar overpressure commonly present in solar thermal systems, the evaporation of heat transfer medium and glycol degradation is suppressed.

In normal operating conditions, the overall efficiency of the thermochromic collectors A1 and A2 is lower than that of a standard collector, due to the somewhat poorer α_{sol} and ε_{th} of 0.84 and 0.09. Assuming a thermochromic collector A3, based on an absorber with a solar absorptance close to that of a standard selective one, α_{sol} = 0.95, but undergoing a thermal emittance modulation as collector A1, a new thermal efficiency curve is simulated. Such a collector A3 would considerably outperform the efficiency of collector A1. In the high temperature state, collector A3 exhibits a similar efficiency curve to collector A1 and yields only slightly higher maximum stagnation temperature of 155°C. The remarkable difference between the two occurs during normal operating conditions, when the efficiency of collector A3, is clearly superior to that of A1 and yields comparable values to that of a standard collector. The efficiency decreases sharply when the thermochromic transition temperature is reached. The thermal efficiency curves of all discussed collector options are displayed in Fig. 3. The efficiency curves and stagnation temperatures for all considered collector types are simulated in SOLCOSI based on measured (A1) or projected (A2 and A3) α_{sol} and ε_{th} values.

Table 2. Calculated stagnation temperatures for flat plate collectors with different absorbers: standard selective, thermochromic A1 (measured) and thermochromic A2 and A3 (projected).

Absorber type	Standard selective	Thermochromic A1 (measured)	Thermochromic A2 (projected)	Thermochromic A3 (projected)
$T_{stagnation}$ [°C]	177	152	147	155

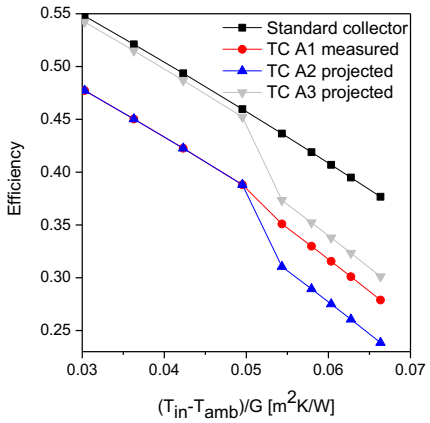

Figure 3. Efficiency curves of a standard flat plate collector and thermochromic collectors based on absorber A1 (measured), A2 and A3 (projected).

4. Conclusions

A multilayered thermochromic absorber A1, based on an Al substrate, a thermochromic VO_2 film, a selective black spinel and an antireflective top layer has been deposited. The thermochromic collector stagnation temperature is expected to be ~25°C lower than that of a standard flat plate collector. This is mostly due to a remarkable increase in thermal emittance above the thermochromic transition, $\Delta\varepsilon = 0.31$, but also to a slightly lower α_{sol} than in a standard absorber. A higher α_{sol} of the thermochromic absorber is desired for higher efficiencies at normal operating temperatures. Moreover, α_{sol} increasing with temperature is also unfavorable and needs to be addressed.

The efficiencies and stagnation temperatures of two thermochromic collectors, A2 and A3 are simulated based on assumed, temperature independent α_{sol} and keeping the same, temperature dependent ε_{th} values as for absorber A1. For a constant solar absorptance of 0.84, as determined for A1 in the low temperature state, the drop in efficiency at the thermochromic phase transition is increased and the lowest stagnation temperature is predicted, $T_{stagnation} = 147$°C. Assuming higher α_{sol} values of 0.95, as customary in standard absorbers, the simulated efficiencies at normal operating temperatures are more adequate, while a rather favorable stagnation temperature of 155°C is reached. However, for best performance in normal operating conditions and enhanced overheating protection, a switch from high to low α_{sol} accompanying the large emittance modulation is desired. In future works, new multilayered designs with improved absorptance in the low temperature state and lower absorptance in the high temperature state shall be proposed.

Acknowledgement

Authors are grateful to Maxime Lagier for his help with sample preparation and to Pierre Loesch for technical support. Financial support for this work was provided by the Swiss Federal Office of Energy (grant no. SI/501239-01).

References

1. A. Paone, M. Joly, R. Sanjines, A. Romanyuk, J.-L. Scartezzini, A. Schüler. Proceedings SPIE 7410, Optical Modeling and Measurements for Solar Energy Systems III, 74100F (2009)
2. A. Krammer, F.T. Demière, A. Schüler. Proceedings of SWC2017 (2017).
3. R. Pérez-Espinosa and O. García-Valladares. J. Renewable Sustainable Energy 10, 013705 (2018).
4. A. Paone, R. Sanjines, P. Jeanneret, A. Schüler. Sol. Energy 118, 107–116 (2015).
5. M. Joly, O. Bouvard, T. Gascou, Y. Antonetti, M. Python, M. A. González Lazo, P. Loesch, A. Hessler-Wyser, A. Schüler. Sol. Energy Mater. Sol. Cells 143, 573–580 (2015).
6. O. García-Valladares and N. Velázquez. Int. J. Heat Mass Transfer 52, 597 (2009).
7. J. Cadafalch, Sol. Energy 83, 2157 (2009).